Z. Phys. C – Particles and Fields 48, 327–339 (1990)

Zeitschrift für Physik C Particles and Fields

Angular correlations for semileptonic D meson decays

G. Köpp[1], G. Kramer[2,*], W.F. Palmer[3,**], G.A. Schuler[2,*]

[1] Physikalisches Institut III A der Rheinisch-Westfälischen Technischen Hochschule, D-5100 Aachen, Federal Republic of Germany
[2] II. Institut für Theoretische Physik der Universität Hamburg, D-2000 Hamburg 50, Federal Republic of Germany
[3] Department of Physics, Ohio State University, Columbus, O 43210, USA

Received 2 May 1990

Abstract. We study the exclusive semileptonic D meson decays $D \to K + \pi + l + \nu$. For this we develop the general formalism for the joint angular distribution of the charged lepton and the K meson and calculate the helicity dependent decay widths which determine the full angular distribution for several models with $K^*(892)$ and $K_0^*(1430)$ intermediate state with nonresonant background terms calculated from chiral Lagrangians.

1 Introduction

In the past the experimental and theoretical study of weak semileptonic decays of hadrons has provided very important information on the structure of the weak current, in particular on its quark structure and on its dependence on the quark mixing parameters. Weak semileptonic decays of mesons containing heavy quarks are of special interest for extracting information on the quark mixing parameters connecting heavy and light quarks. To obtain these parameters from measured branching ratios, lepton spectra or other observables of D and B meson decays we need theoretical input in the form of weak current matrix elements between the initial D or B meson and possible final hadron states. It is clear that the accuracy of such determinations of the weak mixing parameters, in particular of V_{bc} and V_{bu}, depends on the correctness of the theoretical model used to calculate the weak current matrix elements. Therefore it is very important to study these models in such cases where the quark mixing parameter is known, in order to test these models, and, when they fail, to gain insight for their improvement. The decay of D mesons to strange states is such a case since the fact that V_{cs} is almost equal to unity is rather well known. To confront models with a meaningful test it is not sufficient to compare only the branching ratio and the lepton spectrum with experimental data but rather one must make more detailed tests of as many observables as possible. One such possibility is to calculate the angular correlations in the semileptonic decay $D \to K\pi l\nu$, where l may be either an electron or a muon, which arise from lepton–hadron correlations and the angular distribution of the $K\pi$ system in its center of mass frame. The $D \to K\pi l\nu$ decay is dominated by the $K^*(892)$ intermediate state but may have contributions also from $K\pi$ partial waves other than $J^P = 1^-$. It is the purpose of this paper to investigate several models which contain more than just the $K^*(892)$ resonance and calculate the complete differential partial decay width concerning lepton and final meson angles. The angular structure of this partial decay rate is quite similar to K_{l_4} decay which was studied quite extensively many years ago [1]. In contrast to $K \to \pi\pi l\nu$ we have two pseudoscalar mesons with unequal masses in the final state.

The quark model is generally considered to give a reasonable description of the semileptonic decays of heavy quarks, both inclusively [2] and exclusively [3–6]. Quark model calculations agreed reasonably well with the rates for the decays like $D \to Kl\nu$ and with the polarization of the final vector meson in the decay $B \to D^* l\nu$. Recently it became apparent, however, that in the decay of the D meson: $D \to K^* l\nu \to K\pi l\nu$ there is disagreement between the quark model results and the experimental data. First, the measured polarization of the K^* does not agree with the prediction of the quark model. Theoretically the decay widths for transversely and longitudinally produced K^* are almost equal [7–9]. The experiment shows, however, that the K^* is dominantly in a longitudinal state [10]. Second, in the quark model the decay channels $D \to K^* e\nu$ and $D \to Ke\nu$ have comparable rates [7–9] whereas experimentally the rate of $D \to K^* e\nu$ is a factor of two smaller than the rate for $D \to Ke\nu$ [10–11].

Of course it is always possible to fit these experimental data by an adjustment of parameters like overlap integrals for $D \to Kl\nu$ and special form factor fits in $D \to K^* l\nu$ [7, 8, 12]. But the important issue is: are drastic changes of the original quark model calculations necessary or will a fine tuning of the final state hadronization details fit the data? In principle modifications of the

* Supported by Bundesministerium für Forschung und Technologie, 05 4HH92P/3, Bonn, FRG
** Supported in part by the US Department of Energy under contract DE-AC02-76ERO1545

theoretical input can come from two sources. First, the quark model form factors obtained from wave function calculations may differ from the usual results [3–5]. This will modify the predictions for $D \to K l \nu$ and $D \to K^* l \nu$. Second, there may be contributions of other partial waves than the intermediate K^* in $D \to K\pi l\nu$. These other partial wave contributions may originate from nonresonant contributions based on contact terms and off-shell contributions in other channels than $K\pi$, as for example a D^* term in the $D\pi$ channel. Another possibility is that $J^P = 0^+$ and/or 2^+ and/or additional 1^- (with larger masses) resonances in the $K\pi$ channel, although resonating at higher energies, interfere with the dominant K^* terms. It will be difficult to detect such additional terms from rates or electron spectra alone. Since their contributions to the various helicity states of the virtual W (or weak current) will differ from those of the K^* terms it is of interest to study the joint angular distribution of the K (or π) meson and the lepton $l^\pm$. This will permit the detection of additional $K\pi$ partial waves and/or background terms and will also help to determine the relative signs and form factors of the dominant K^* intermediate state [12–14].

A model for the nonresonant background contribution has been developed recently by two of us and J. Cline [7]. In this work weak transition amplitudes of the D meson to two pseudoscalar mesons have been written down which have the same structure concerning transitions to resonant vector meson states as the usual quark model approaches [3–6], but have in addition the constraints arising from low-energy theorems codified in the chiral Lagrangian [15]. The low-energy constraints lead to additional terms which produce the nonresonant background underneath the dominant resonant contribution. For the additional resonances at higher masses we shall make an ansatz for a scalar resonance at $m = 1.429\,\mathrm{GeV}$ [16] with an arbitrary parameter for its strength.

In Sect. 2 we derive the complete formula of the differential decay distribution for $D \to K\pi e\nu$ and present the partial wave expansion of the occurring helicity amplitudes. Section 3 contains the weak currents for the model of the K^* resonance with background and 0^+ contribution from which the form factors needed for calculating the angular correlation coefficients are derived. In Sect. 4 we present our numerical results for the coefficient functions of the lepton angular correlation. Here we study the influence of the background terms and the 0^+ contribution. In Appendix A we collect some material for deriving the angular distribution and in Appendix B we consider modifications for the case that the charged lepton mass is nonzero which are relevant for $D \to K\pi\mu\nu$ decays.

2 Semileptonic decay angular distribution

Following earlier work [15] we write the total semileptonic decay rate as

$$\Gamma = \frac{2G_F^2 |V_{cs}|^2}{m_1 (2\pi)^2} \int \frac{d^3k}{2k_0} \frac{d^3k'}{2k'_0} H^{\mu\nu} l_{\mu\nu} \tag{1}$$

with the lepton tensor

$$l_{\mu\nu} = k_\mu k'_\nu + k'_\mu k_\nu - k'k g_{\mu\nu} + i\varepsilon_{\mu\nu\alpha\beta} k^\alpha k'^\beta \tag{2}$$

and the hadron tensor

$$H_{\mu\nu} = \sum_X \int \frac{d^3p_2}{2p_{20}} \frac{d^3p_3}{2p_{30}} \frac{1}{(2\pi)^6} \delta^{(4)}(p_1 - q - p_2 - p_3) \tag{3}$$

$$\langle D(p_1)|J^\dagger_\mu(q)|X(p_2,p_3)\rangle \langle X(p_2,p_3)|J_\nu(q)|D(p_1)\rangle.$$

V_{cs} denotes the Kobayashi–Maskawa matrix element for the transition from charm to strange quarks. The momenta correspond to the process

$$p_1 \to p_2 + p_3 + k + k' \tag{4}$$

where p_2 and p_3 are the momenta of the K and π, respectively, k is the electron momentum, k' is the neutrino momentum, $q = k + k'$ the momentum transfer to the lepton system and m_1 the mass of the decaying D meson. In the following we shall neglect the mass of the electron. Effects of a finite lepton mass which are of interest for the decay into muons will be considered separately in Appendix B.

The full differential decay distribution $d\Gamma$ is a function of five configuration variables. If these variables are properly chosen the dependence on two of these variables is quite explicit and can be factored out. This follows from the factorization of the lepton tensor as we shall see below. The situation is completely analogous to the treatment of K_{l_4} decay many years ago [1]. The essential dynamical effects are contained in certain form factors which can depend at most on the remaining three of the five variables. To derive this dependence on the lepton variables we express the lepton tensor in terms of nine independent basis tensors $L^{(i)}_{\mu\nu}(i = U, L, T, V, F, I, P, A, N)$ which are defined in terms of polarization tensors

$$L^{\rho\sigma}_{\mu\nu} = \varepsilon_\mu(q,\rho)\varepsilon^*_\nu(q,\sigma). \tag{5}$$

In (5) the $\varepsilon^\mu(q,\lambda)$ are the polarization vectors of the virtual W (or lepton current) with polarization $\lambda = \pm 1, 0, s$. The polarization vectors are specified in the rest system of the virtual W: $\mathbf{q} = 0$, where $\varepsilon^\mu(q,\pm 1) = \mp(0,1,\mp i,0)/\sqrt{2}$, $\varepsilon^\mu(q,0) = (0,0,0,-1)$, $\varepsilon^\mu(q,s) = q^\mu/\sqrt{q^2}$, $q^\mu = (q^0,0,0,0)$. The scalar (zero) helicity component of the $W, \lambda = s$, contributes only if the lepton mass is nonvanishing. It is included in (5) for application in Appendix B. For $\rho, \sigma = \pm 1, 0$ the tensor $L_{\mu\nu}(\rho,\sigma)$ has no time components. In the system $\mathbf{q} = 0$ and for vanishing lepton mass, $l_{\mu\nu}$ has also only space components, $\mu, \nu = 1,2,3$. The lepton tensor is hermitean $l_{\mu\nu} = l^\dagger_{\mu\nu}$. Therefore it can be expressed in terms of nine independent basis tensors as follows

$$l_{\mu\nu} = \frac{2q^2}{3}\{l_U L^{(U)}_{\mu\nu} + l_L L^{(L)}_{\mu\nu} + l_T L^{(T)}_{\mu\nu} + l_V L^{(V)}_{\mu\nu} + l_F L^{(F)}_{\mu\nu} + l_I L^{(I)}_{\mu\nu}$$
$$+ l_P L^{(P)}_{\mu\nu} + l_A L^{(A)}_{\mu\nu} + l_N L^{(N)}_{\mu\nu}\}. \tag{6}$$

The basis tensors are simple matrices in $\mu, \nu = 1,2,3$. They are written down in Appendix A and are expressed in terms of the polarization tensors (5)

$$L^{(U)} = L^{++} + L^{--} \qquad L^{(F)} = (L^{+0} - L^{0+} + L^{-0} - L^{0-})/4i$$
$$L^{(L)} = L^{00} \qquad L^{(I)} = (L^{+0} + L^{0+} - L^{-0} - L^{0-})/4$$

$$L^{(T)}=(L^{+-}+L^{-+})/2 \quad L^{(N)}=(L^{+0}-L^{0+}+L^{0-}-L^{-0})/4i$$
$$L^{(V)}=(L^{+-}-L^{-+})/2i \quad L^{(A)}=(L^{+0}+L^{0+}+L^{-0}+L^{0-})/4$$
$$L^{(P)}=L^{++}-L^{--}. \tag{7}$$

The coefficient functions l_U, l_L, l_T, etc. are easily calculated in terms of the angles θ and χ which specify the lepton momenta k and k' in the current rest system $\mathbf{q}=0$ with respect to the coordinate system shown in Fig. 1a and described later. In terms of these angles we have

$$k^\mu = k^0(1, \sin\theta\cos\chi, \sin\theta\sin\chi, \cos\theta) \tag{8}$$

and $k'^\mu = q^\mu - k^\mu$, $k^0 = \sqrt{q^2}/2$. The coefficients l_U, l_L, l_T, etc. are written down later as functions of θ and χ. The dependence on q^2 together with a common normalization factor has been factored out already in (6). The decomposition (6) allows us to replace the tensor product $l^{\mu\nu}H_{\mu\nu}$ by the coefficient functions l_U, l_L, l_T, etc. and helicity structure functions H_i which depend on the polar angle of the K meson θ^* and the $(K\pi)$-invariant mass squared $s_{23}=(p_2+p_3)^2$. The H_i are:

$$H_i = L^{(i)}_{\mu\nu}H^{\mu\nu} \quad (i=U,L,T,V,F,I,P,A,N). \tag{9}$$

With these definitions we obtain for the differential decay distribution with respect to $q^2, \cos\theta$ and χ:

$$\frac{2\pi d^3\Gamma}{dq^2 d\cos\theta d\chi} = \frac{G_F^2|V_{cs}|^2 q^2}{96(2\pi)^5 m_1^3}\int_{(m_2+m_3)^2}^{(m_1-\sqrt{q^2})^2} ds_{23}\int_{-1}^{+1} \cdot d\cos\theta^* \sqrt{a_2}\, X\, l^{\mu\nu}H_{\mu\nu} \tag{10}$$

where

$$l_{\mu\nu}H^{\mu\nu} = l_U H_U + l_L H_L + l_T H_T + l_V H_V + l_F H_F + l_I H_I + l_P H_P + l_A H_A + l_N H_N \tag{11}$$

with

$$l_U = \frac{3}{8}(1+\cos^2\theta) \qquad l_F = \frac{3}{2\sqrt{2}}\sin 2\theta\sin\chi$$
$$l_L = \frac{3}{4}\sin^2\theta \qquad l_I = -\frac{3}{2\sqrt{2}}\sin 2\theta\cos\chi$$
$$l_T = \frac{3}{4}\sin^2\theta\cos 2\chi \qquad l_N = \frac{3}{\sqrt{2}}\sin\theta\sin\chi$$
$$l_V = -\frac{3}{4}\sin^2\theta\sin 2\chi \qquad l_A = -\frac{3}{\sqrt{2}}\sin\theta\cos\chi$$
$$l_P = \frac{3}{4}\cos\theta \tag{12}$$

and

$$H_U = H^{++} + H^{--}$$
$$H_F = \frac{-i}{4}(H^{+0} - H^{0+} + H^{-0} - H^{0-})$$
$$H_L = H^{00}$$
$$H_I = \tfrac{1}{4}(H^{+0} + H^{0+} - H^{-0} - H^{0-})$$
$$H_T = \tfrac{1}{2}(H^{+-} + H^{-+})$$
$$H_A = \tfrac{1}{4}(H^{+0} + H^{0+} + H^{-0} + H^{0-})$$
$$H_V = \frac{-i}{2}(H^{+-} - H^{-+})$$
$$H_N = \frac{-i}{4}(H^{+0} - H^{0+} - H^{-0} + H^{0-})$$
$$H_P = H^{++} - H^{--}. \tag{13}$$

It follows from (10) and (11) that the dependence on the electron angles factors out completely and is given by the simple coefficients in (12). If the complete angular dependence could be measured, all nine structure functions $d^3\Gamma_i$ could be determined:

$$\frac{d^3\Gamma_i}{dq^2 ds_{23} d\cos\theta} = \frac{G_F^2|V_{cs}|^2 q^2\sqrt{a_2}X}{96(2\pi)^5 m_1^3}H_i \tag{14}$$

where $i=U,L,T,V,F,I,P,A,N$ so that the fully differential decay distribution is:

$$\frac{2\pi d^5\Gamma}{dq^2 d\cos\theta d\chi ds_{23} d\cos\theta^*} = \sum_i l_i \frac{d^3\Gamma_i}{dq^2 ds_{23} d\cos\theta^*} \tag{15}$$

with the lepton coefficients given in (12). As mentioned earlier the dependence on the lepton angles θ and χ is completely trivial and factors out. The dynamics of the decay is contained in the structure functions H_i. They depend on $s_{23}, \cos\theta^*$ and q^2. In (10) and (14) we defined $X = \sqrt{s_{23}}|\mathbf{q}| = \sqrt{s_{23}}|\mathbf{p}_1| = \lambda^{1/2}(m_1^2, s_{23}, q^2)/2$ and $\sqrt{a_2} = 2|\mathbf{p}_2|/\sqrt{s_{23}} = 2|\mathbf{p}_3|/\sqrt{s_{23}} = \lambda^{1/2}(s_{23}, m_2^2, m_3^2)/s_{23}$. They are related to the momenta of the D and the K meson in the $K\pi$ rest system $\mathbf{P}=\mathbf{p}_2+\mathbf{p}_3=0$ (we use $P=p_2+p_3$ in the following). The structure functions H_i can be calculated from the decomposition of the hadronic matrix element. This has an axial-vector and a vector part with the following structure

$$J_\mu \equiv \langle p_2, p_3 | A_\mu + V_\mu | p_1\rangle = \frac{1}{m_1}\left[f(p_2+p_3)_\mu + g(p_2-p_3)_\mu + rq_\mu + \frac{ih}{m_1^2}\varepsilon_{\mu\nu\alpha\beta}q^\nu(p_2+p_3)^\alpha(p_2-p_3)^\beta\right]. \tag{16}$$

The first three terms come from the axial-vector part, the last term from the vector part. The dimensionless form factors f, g, r and h are functions of the invariant variables s_{23}, q^2 and of θ^*. The term proportional to r does not contribute for vanishing lepton mass since $q^\mu l_{\mu\nu}=0$. The ansatz (16) is the most general one. This means that the decay distributions are known if the complex functions f, g and h are given. The next step is to express the structure functions H_i in (13) by the functions f, g and h. For this purpose we calculate the helicity projections of the currents, $\varepsilon_\mu^*(q,\rho)J^\mu$ for $\rho=\pm 1, 0$ in the coordinate system $\mathbf{P}=0$, i.e. in the $K\pi$ rest system. For this we need the polarization vectors of the virtual W in this system, which are obtained through a boost from the polarization vectors in the W rest system. The coordinates in the $K\pi$ rest system are chosen in such a way that the z-axis is along the momentum $\mathbf{P}$ in the rest system $\mathbf{p}_1=0$ (see Fig. 1a) and that the K momentum lies in the x–z-plane with positive x component. The angle θ^* is

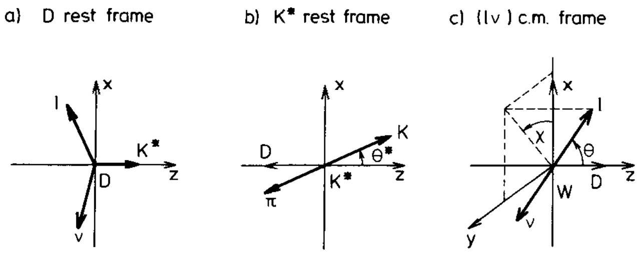

Fig. 1 a–c. Direction of momenta in various frames **a** D rest frame, **b** θ^* in $(K\pi)$ c.m. frame, **c** θ and χ in $(l\nu)$ c.m. frame

specified in the $K\pi$ rest frame (see Fig. 1b) which is obtained from D and W rest frames by boosts along the momentum $\mathbf{P}$, i.e. $p_2^\mu=(p_{20},|\mathbf{p}_2|\sin\theta^*,0,|\mathbf{p}_2|\cos\theta^*)$ with $p_{20}=(s_{23}+m_2^2-m_3^2)/(2\sqrt{s_{23}})$ and $|\mathbf{p}_2|=\sqrt{s_{23}}\sqrt{a_2}/2$. The azimuthal angle χ is the angle between the $W\to e\nu$ decay plane and the plane defined by the vectors $\mathbf{p}_2$ and $\mathbf{p}_3$ in frame (a) or (b) of Fig. 1. θ is the polar angle of the charged lepton with respect to the z-axis chosen along the $K\pi$ momentum in the current rest frame where the x–z plane is chosen as the virtual W decay plane with $k_x>0$ (see Fig. 1c). Then the boosted W polarization vectors have the following form:

$$
\begin{aligned}
\varepsilon(q,\pm)^\mu &= \mp\frac{1}{\sqrt{2}}(0,1,\mp i,0)\\
\varepsilon(q,0)^\mu &= \frac{1}{\sqrt{q^2}}(|\mathbf{q}|,0,0,-q^0)\\
\varepsilon(q,s)^\mu &= \frac{1}{\sqrt{q^2}}q^\mu=\frac{1}{\sqrt{q^2}}(q^0,0,0,-|\mathbf{q}|)
\end{aligned}
\tag{17}
$$

with $|\mathbf{q}|=|\mathbf{p}_1|=X/\sqrt{s_{23}}$ where $p_1^\mu=(p_{10},0,0,-|\mathbf{p}_1|)$ and $q_0=Pq/\sqrt{s_{23}}$, $Pq=(m_1^2-s_{23}-q^2)/2$, $p_{10}=q_0+\sqrt{s_{23}}$, and the helicity projections of J_μ in the system $\mathbf{P}=0$ are:

$$
\begin{aligned}
F_0 &= \varepsilon^*(q,0)_\mu J^\mu\\
&= \frac{1}{m_1\sqrt{q^2}}\left[X\left(f+\frac{m_2^2-m_3^2}{s_{23}}g\right)+g\sqrt{a_2}Pq\cos\theta^*\right]\\
F_\pm &= \varepsilon^*(q,\pm)_\mu J^\mu=\pm\frac{\sqrt{a_2 s_{23}}}{m_1\sqrt{2}}\left[g\pm\frac{hX}{m_1^2}\right]\sin\theta^*.
\end{aligned}
\tag{18}
$$

The projection $\varepsilon^*(q,s)_\mu J^\mu$ is not needed. It will be given in Appendix B for calculating lepton mass effects. The functions F_λ $(\lambda=0,\pm 1)$ are the helicity amplitudes in the frame $\mathbf{P}=0$. They have the following partial wave expansion:

$$
F_\lambda=\sum_j(2j+1)d^j_{\lambda,0}(\theta^*)F^j_\lambda. \tag{19}
$$

We have $d^j_{0,0}(\theta)=P_j(\cos\theta)$ and $d^j_{\pm 1,0}=\mp\sin\theta P'_j(\cos\theta)/\sqrt{j(j+1)}$. This means that the expansion of F_0 starts with $j=0$ whereas for $F_{\pm 1}$ the lowest partial wave is $j=1$. The partial wave amplitudes F^j_λ, which depend only on s_{23} and q^2 have the final state interaction phases δ_j for $I=1/2$ $K\pi$ scattering. The phase shifts depend on the single variable s_{23}. The main contribution to F_λ comes from the intermediate state $K^*(892)$ resonance which is purely elastic. It will be considered in more detail in the next section. If we restrict the expansion (19) to s- and p-waves only then the form factors g and h are independent of θ^* whereas f is at most linear in $\cos\theta^*$. The s-wave is resonant at $\sqrt{s_{23}}=1.429\,\text{GeV}$ yielding the $K_0^*(1430)$ state which also decays dominantly into $K\pi$. It has a rather large width of $(0.287\pm 0.023)\,\text{GeV}$. From threshold the phase shift δ_0 grows monotonically with energy until it reaches 90° near the resonance mass [17]. In all helicity cross sections H_i which involve F_0, i.e. H_L, H_F, H_I, H_A and H_N (see (13)), we expect strong interference terms between $j=0$ and $j=1$ contributions. Therefore these cross sections would be ideal for studying the phase difference $\delta_0-\delta_1$ in isodoublet $K\pi$ scattering. Other resonances that might contribute are $K^*(1415)$, which however decays dominantly into $K^*\pi$, and $K_2^*(1430)$ with $j=2$.

To facilitate the evaluation of the partial cross sections proportional to H_i for particular models, which will be done in the next section, we exhibit the dependence of the H_i on the form factors f, g and h. Substituting the expressions for F_λ given in (18) into the general formulas (13) we obtain

$$
\begin{aligned}
H_U &= C_1\left(|g|^2+\frac{|h|^2X^2}{m_1^4}\right)\\
H_L &= \frac{1}{q^2m_1^2}|Xf+C_2g|^2\\
H_T &= \frac{-1}{2}C_1\left(|g|^2-\frac{|h|^2X^2}{m_1^4}\right)\\
H_V &= \frac{-X}{m_1^2}C_1\Im\{h^*g\}\\
H_F &= \frac{X}{m_1^2}C_3\Im\{h^*[Xf+C_2g]\}\\
H_I &= C_3\Re\{g^*[Xf+C_2g]\}\\
H_P &= \frac{2X}{m_1^2}C_1\Re\{g^*h\}\\
H_A &= \frac{X}{m_1^2}C_3\Re\{h^*[Xf+C_2g]\}\\
H_N &= C_3\Im\{g^*Xf\}
\end{aligned}
\tag{20}
$$

where $\Re$ and $\Im$ denote real and imaginary part and where we defined

$$
\begin{aligned}
C_1 &= \frac{a_2s_{23}}{m_1^2}\sin^2\theta^*\\
C_2 &= \kappa X+\sqrt{a_2}\frac{m_1^2-s_{23}-q^2}{2}\cos\theta^*\\
C_3 &= \frac{\sqrt{a_2s_{23}}}{\sqrt{2q^2m_1^2}}\sin\theta^*\\
\kappa &= \frac{m_2^2-m_3^2}{s_{23}}.
\end{aligned}
\tag{21}
$$

We notice that as long as we restrict the partial wave expansion (19) to s- and p-waves the cross sections H_U, H_T, H_V and H_P depend on θ^* only through the characteristic multiplicative factor $\sin^2\theta^*$ and give information on the $J^P = 1^-$ states only. All the other cross sections involve s–p interference. Obviously H_L, H_I and H_A depend on the s–p phase shift difference in the form $\cos(\delta_0 - \delta_1)$ whereas H_F and H_N are proportional to $\sin(\delta_0 - \delta_1)$.

In the next section we shall present the form factors f, g and h for several models including the simplest one, which has only the $K^*(892)$ as intermediate $K\pi$ state.

3 Resonance model with background

From the available experimental data it is not yet clear that the $K^*(892)$ resonance is the only contribution in D^0 and D^+ decays to the $K\pi l\nu$ final state. MARK III reports for the ratio of resonant to nonresonant contribution in D^0 decays the number 4.0/1.9 and in D^+ decays 2.9/1.3 [11] whereas in the E691 experiment these numbers are 1.7/0.3 and 4.5/0.3 [18]. Thus the E691 experiment finds far less nonresonant background than the MARK III collaboration. It is hoped that the other partial decay rates if measured will give better data on the nonresonant terms than the total decay rate.

To get an idea how the other partial decay rates $d\Gamma_i (i = U, L, T,$ etc.) look like we shall investigate a model that consists of the $K^*(892)$ intermediate state, where the finite width is fully taken into account, and an additional background term which is motivated by an effective chiral Lagrangian approach including a Wess–Zumino term. This model is described in detail in earlier work [7]. From this we can read off the form factors f, g and h for this particular model which are then substituted into (20). To clarify the notation we shall repeat the main formulas from [7].

For the hadronic form factors f, g, h for the transition to two pseudoscalar mesons we consider, to be specific, the process $D^+ \to K^- + \pi^+ + e^+ + \nu$. The effective Lagrangian approach yields the following expression for J_μ which is valid at threshold and in the limit of $SU(4)$ chiral symmetry [15]

$$J_\mu = \frac{2\sqrt{2}}{\pi^2 F_\pi^3} \varepsilon_{\mu\nu\alpha\beta} p_3^\nu p_2^\alpha p_1^\beta G_V(q^2) + \frac{i2\sqrt{2}}{3F_\pi}(2p_3 + p_1 - p_2)^\nu \cdot \left[g_{\mu\nu} G_A(q^2) - \frac{q_\mu q_\nu}{q^2 - m_F^2} \right] \tag{22}$$

where G_V and G_A describe the q^2 pole behaviour of the weak vector and axial-vector current. The $q_\mu q_\nu$ term does not contribute for vanishing lepton mass. We now add renonance terms in the two-body pseudoscalar channels. The vector current $V_\mu (J_\mu = V_\mu + A_\mu)$ is given by

$$V_\mu = \frac{2\sqrt{2}}{\pi^2 F_\pi^3} \varepsilon_{\mu\nu\alpha\beta} p_3^\nu p_2^\alpha p_1^\beta \frac{1}{2} G_V \cdot \left\{ I_b^V \frac{m_{D^*}^2}{m_{D^*}^2 - s_{13}} + (I_b^V - I f_V) + I f_V \frac{m_{K^*}^2 - i m_{K^*}\Gamma}{m_{K^*}^2 - s_{23} - i m_{K^*}\Gamma} \right\} \tag{23}$$

and the axial-vector part A_μ is

$$A_\mu = \frac{i2\sqrt{2}}{3F_\pi} \Bigg\{ (I_b^V - I f_A)(p_3 - p_2)_\mu + I f_A \frac{m_{K^*}^2 - i m_{K^*}\Gamma}{m_{K^*}^2 - s_{23} - i m_{K^*}\Gamma} \cdot \Bigg[(p_3 - p_2)_\mu + \hat{\kappa}(p_3 + p_2)_\mu + \frac{F_2^A(0)}{F_1^A(0)} p_{1\mu}[p_1(p_3 - p_2) + \hat{\kappa} p_1(p_2 + p_3)] \Bigg] + I_b^V \frac{m_{D^*}^2}{m_{D^*}^2 - s_{13}}(p_1 + p_3)_\mu \Bigg\} G_A \tag{24}$$

with

$$s_{13} = m_1^2 + m_3^2 - \left(\frac{(s_{23} + m_1^2 - q^2)(s_{23} + m_3^2 - m_2^2)}{2s_{23}} - \sqrt{a_2} X \cos\theta^* \right)$$

$$\hat{\kappa} = \frac{m_2^2 - m_3^2}{m_{K^*}^2}. \tag{25}$$

In (22), (23) and (24) F_π is the pion decay constant $F_\pi = 0.18\,\text{GeV}$. The terms proportional to $m_2^2 - m_3^2$ are needed for the correct spin projection of the intermediate vector state. In (23) and (24) the parameters f_V and f_A decouple the resonance enhancement of the K^* from the low energy behaviour. Without them, i.e. for $f_V I = f_A I = 1$, relations between different coupling constants evolve which are in disagreement with experiment (for more discussion on this point see [19]). f_V and f_A parametrize the possibility that this decoupling is different for vector and axial-vector currents. I stands for overlap integrals for the transition $D \to K^*$ which are assumed to be equal for the vector and the axial-vector current. I_b^V and I_b^A have been introduced to account for chiral symmetry violations of the contact term and the D^* exchange term. They will be specified in the next section in such a way that they approach $I_b^{V,A} = 1$ in the chiral symmetry limit. Then in this limit (23) and (24) reduce to (22) when s_{13} and s_{23} are evaluated at soft threshold $s_{13} = s_{23} = 0$ and $m_1 = m_2 = m_3 = 0$ for any value of the parameters f_V and f_A. We have not modified the D^* pole term in the same way as the K^* pole with threshold and pole enhancement decoupled and also have not included the term to ensure the correct spin projection for a vector particle. The D^* pole is off-shell and becomes essentially part of the contact term. Since s_{13} depends on θ^* it contains all partial waves in the $K\pi$ channel. The D^* pole terms along with terms proportional to $(I_b^{V,A} - I f_{V,A})$ describe our nonresonant background contributions which are motivated by chiral symmetry and crossing symmetry. We note that the term proportional to F_2^A are irrelevant at the threshold point. The form factors F_1^A, F_2^A and F^V are the transition form factors for $D \to K^* e\nu$ in zero-width approximation. They are defined in the previous paper [7] and are identical to the notation of [6]. We can relate them to f_V, f_A, I and the coupling constant for the decay $K^{*0} \to K^- \pi^+$ as follows:

$$f_A = \frac{3\sqrt{2} g_{K^{*0}K^-\pi^+} F_\pi F_1^A(0)}{4 m_{K^*}^2 I}$$

$$f_V = \frac{\pi^2 F_\pi^2 \sqrt{2} g_{\bar{K}^{*0}K^-\pi^+} F_\pi F^V(0)}{m_{K^*}^2 I} \tag{26}$$

where $g_{\bar{K}^{*0}K^-\pi^+}$ is related to the K^* width via

$$g_{\bar{K}^{*0}K^-\pi^+} = \sqrt{\frac{4\pi \Gamma_{K^*} m_{K^*}^2}{p^3}}$$
$$p^2 = \frac{\lambda(m_{K^*}^2, m_2^2, m_3^2)}{4m_{K^*}^2}. \tag{27}$$

The $F_1^A(0), F_2^A(0)$ and $F^V(0)$ are adjusted to the values as used by Körner and Schuler [6] who matched the spin properties of the mesonic transitions to the free quark decay transitions at $q^2 = 0$ which yields

$$F_1^A(0) = I(m_1 + m_{K^*})$$
$$F_2^A(0) = R_{12} \frac{-2I}{m_1 + m_{K^*}}$$
$$F^V(0) = R_V \frac{2I}{m_1 + m_{K^*}}. \tag{28}$$

The overlap factor I stands for deviations from the matching to the free quark model and is not in this work assumed to be universal for all three form factors. Thus we include the relative strength factors R_{12} and R_V. A value for these overlap factors will be specified later together with our assumptions on the q^2 behaviour of $G_V(q^2)$ and $G_A(q^2)$ in (23) and (24). Finally we mention that actually there is no reason to multiply the contact term, i.e. the first two terms in (23) and the first and the last term in (24) with the same q^2 dependent form factors G_V and G_A as the terms describing the $D \to K^*$ transition. We shall make this assumption, however, for lack of better knowledge.

From (23) and (24) we can read off the expressions for the functions f, g and h for the resonance and background model. They are:

$$f = iK_1 \left(If_A \,\mathrm{Res}(K^*) \left[\hat{\kappa} + \frac{F_2^A(0)}{F_1^A(0)} B_0 \right] + \frac{3}{2} I_b^A \,\mathrm{Res}(D^*) \right)$$
$$g = -iK_1 \left([I_b^A - If_A] + If_A \,\mathrm{Res}(K^*) + \frac{1}{2} I_b^A \,\mathrm{Res}(D^*) \right)$$
$$h = iK_2([I_b^V - If_V] + If_V \,\mathrm{Res}(K^*) + I_b^V \,\mathrm{Res}(D^*)). \tag{29}$$

Here we have defined

$$K_1 = \frac{2\sqrt{2} m_1 G_A}{3F_\pi}$$
$$K_2 = -\frac{\sqrt{2} m_1^3 G_V}{2F_\pi^3 \pi^2}$$
$$B_0 = p_1(p_3 - p_2) + p_1(p_2 + p_3)\hat{\kappa}. \tag{30}$$

The resonance terms are defined as follows:

$$\mathrm{Res}(K^*) = \frac{m_{K^*}^2 - i m_{K^*} \Gamma_{K^*}}{m_{K^*}^2 - s_{23} - i m_{K^*} \Gamma_{K^*}}$$
$$\mathrm{Res}(D^*) = \frac{m_{D^*}^2}{m_{D^*}^2 - s_{13}}. \tag{31}$$

Since

$$B_0 = -\sqrt{a_2} X \cos\theta^* + \hat{\kappa} \frac{m_1^2 + s_{23} - q^2}{2} \frac{s_{23} - m_{K^*}^2}{s_{23}} \tag{32}$$

we note that on the basis of (18) and (19) the terms proportional to $\mathrm{Res}(K^*)$ contribute at resonance only to the p-wave amplitude in F_0, as it should be. So far any s-wave term in F_0 can come only from the term proportional to $\mathrm{Res}(D^*)$ in f.

It is well known that there are other resonant $K\pi$ states at higher masses which could interfere with the dominant $K^*(892)$ resonance. In order to test such a possibility we consider a contribution from the $K_0^*(1430)$ resonance, which decays dominantly into $K\pi$ with a rather large total width $\Gamma = 0.287$ GeV. The matrix element of the weak current between the D meson and the K_0^* is unknown. Such a resonance can only contribute to f. For this additional resonance term we make the ansatz

$$f \to f + iK_1[-\varepsilon If_A + \varepsilon If_A \,\mathrm{Res}(K)]$$
$$= iK_1 \left(If_A \,\mathrm{Res}(K^*) \left[\hat{\kappa} + \frac{F_2^A(0)}{F_1^A(0)} B_0 \right] + \frac{3}{2} I_b^A \,\mathrm{Res}(D^*) - \varepsilon If_A + \varepsilon If_A \,\mathrm{Res}(K) \right) \tag{33}$$

where the parameter ε measures the strength of this resonance compared to the dominant $K^*(892)$ resonance and

$$\mathrm{Res}(K) = \frac{m_K^2 - i m_K \Gamma_K}{m_K^2 - s_{23} - i m_K \Gamma_K}. \tag{34}$$

We shall calculate the partial cross section for several values of ε and also look at the s_{23} spectrum of the integrated semileptonic decay width. Of course other resonance contributions could be introduced. If they have higher spins then we need more than one parameter to parametrize their contribution.

All our formulas and the results in the next section are for $(l^+ \nu_l)$ emission. The $(l^- \bar{\nu}_l)$ emission case is obtained by changing the sign of l_P, l_N and l_A in (15) and changing the sign of the form factor h in (20). Therefore the angular coefficients of the CP-odd terms, V, F and N change sign. These are the odd terms proportional to $\sin\chi$ and $\sin 2\chi$ in the χ distribution, which cancel if the decays of D and $\bar{D}$ are averaged.

4 Numerical results

For illustrative purposes, we will present numerical results choosing input parameters for two basic cases. The first is suggested by a recent result reported for the ratio of longitudinal to unpolarized transverse decay [21]. The second is for the quark model parameterization of Körner and Schuler [6]. No experimental cuts have been made. Complete results are given only for the first case. These numerical results are only to illustrate the variations one can expect from various models; we are not attempting to fit data or claim a superiority of one set of input parameters over another. Current data is too crude to distinguish among the sets. Only better data combined with acceptance corrections and a sophisticated fitting procedure will nail down the models.

We assume the following q^2 behaviour of G_V and G_A

$$G_V(q^2)=\frac{m_{D_s^*}^2}{m_{D_s^*}^2-q^2}$$
$$G_A(q^2)=\frac{m_{D_A^*}^2}{m_{D_A^*}^2-q^2}. \tag{35}$$

Furthermore we define

$$I_b^V=\frac{m_{D_s^*}^2-(m_D-m_K-m_\pi)^2}{m_{D_s^*}^2}$$
$$I_b^A=\frac{m_{D_A^*}^2-(m_D-m_K-m_\pi)^2}{m_{D_A^*}^2}. \tag{36}$$

If the factors $I_b^{V,A}$ and $G_{V,A}$ are combined we obtain the following form factors of the contact terms and the D^* exchange term

$$\hat{G}_V(q^2)=\frac{m_{D_s^*}^2-(m_D-m_K-m_\pi)^2}{m_{D_s^*}^2-q^2}$$
$$\hat{G}_A(q^2)=\frac{m_{D_A^*}^2-(m_D-m_K-m_\pi)^2}{m_{D_A^*}^2-q^2}. \tag{37}$$

$I_b^{V,A}$ have the property that they are equal to one for $m_D=m_K=m_\pi=0$. Independent of the pseudoscalar masses, the form factors of the contact terms in (37) approach unity at the q^2 threshold $q^2=(m_D-m_K-m_\pi)^2$ where the recoiling final two-meson system is at rest.

The parameters are choosen as follows:

$$\begin{aligned}
m_D &\equiv m_1 = 1.8693\,\text{GeV}\\
m_K &\equiv m_2 = 0.4937\,\text{GeV}\\
m_\pi &\equiv m_3 = 0.13957\,\text{GeV}\\
m_{K^*} &= 0.8921\,\text{GeV}\\
m_{D^*} &= 2.010\,\text{GeV}\\
m_{D_s^*} &= 2.113\,\text{GeV}\\
m_{D_A^*} &= 2.54\,\text{GeV}\\
\Gamma_{K^*} &= 0.0513\,\text{GeV}\\
m_{K_0^*} &= 1.429\,\text{GeV}\\
\Gamma_{K_0^*} &= 0.287\,\text{GeV}\\
F_\pi &= 0.180\,\text{GeV}\\
I &= 0.5\\
R_{12} &= 0\\
R_V &= 1.86.
\end{aligned} \tag{38}$$

Except for the last four input numbers all others are taken from the Particle Data Group tables [16]. We have chosen $R_{12}=0$ and $R_V=1.86$ in order to reproduce a new value for the ratio of the longitudinal to the unpolarized transverse decay rate [20], which differs somewhat from the earlier published value [10]. $I=0.5$ accounts for the correct absolute value of the semileptonic decay rate into $K\pi e\nu$ [18]. For the form factor mass in the axial-vector current we used the recently measured value [21].

First we show our results for the integrated partial decay rates. For this we have integrated the decay distributions $d^3\Gamma_i$ in (14) for $i=U,L,T,V,I,P,A,N$ over the meson angle θ^*, s_{23} and q^2. The result for the five models, namely i) the model with a pure $K^*(892)$ resonance (in zero-width approximation and with the full width taken into account), ii) the model with the D^* pole term added to the full width model, iii) the model with D^* and all other contact terms added ($\varepsilon=0$) and iv) and v) the model with the additional s-wave resonance (K_0^*) term added for two strength parameters $\varepsilon=-1$ and $\varepsilon=+1$ are collected in Table 1. All rates are for the sum of both final charge states, i.e. for D^0 decays $D^0\to K^-\pi^0e^+\nu$ and $D^0\to\bar{K}^0\pi^-e^+\nu$. Therefore the formulas in Sect. 2 have been multiplied by 1.5. The partial rates Γ_V, Γ_F and Γ_N obtained from the imaginary part of the product of amplitudes f, g and h vanish for the pure resonance model. Furthermore in this model the integrands of Γ_A and Γ_I have the factor $\sin 2\theta^*$. Therefore they vanish after integration over the total θ^* range. We see this is the case for the K^* model in zero-width approximation. In the model with the full width taken into account we obtain small values for Γ_A and Γ_I since they have small off-mass-shell terms proportional to $s_{23}-m_{K^*}^2$ included in (20) with f, g and h as given in (29). The factor $\sin 2\theta^*$ is also present in Γ_F and Γ_N. To remedy this drawback we have calculated also moments of $\sin 2\theta^*$ for $\Gamma_F, \Gamma_I, \Gamma_A$ and Γ_N, i.e. we integrated $\sin 2\theta^* d^3\Gamma_i (i=F,I,A,N)$. The results for these moments are denoted $F\sin 2\theta^*$ etc. in Table 1. We see now that $I\sin 2\theta^*$ and $A\sin 2\theta^*$ are not zero or very small for the pure resonance model.

As we shall comment upon again below, the angular distribution in the hadron angle θ^* has the simple form $1+\alpha\cos^2\theta^*$ only in the pure K^* resonance model in narrow width. In this kind of model, to which data are usually fit, the ratio of longitudinal to transverse unpolarized decay rate is:

$$\Gamma_L/\Gamma_U=(1+\alpha)/2. \tag{39}$$

For this reason we quote the value of $(1+\alpha)/2$ as well as Γ_L/Γ_U in our numerical results.

Now let us compare the results of the various models as given in Table 1. In all models the longitudinal decay rate Γ_L is dominant. This has its origin in our choice $F_2^A=0$ (see (38)). In fact we have fixed I, R_{12} and R_V so that we agree with recent preliminary data of experiment E691, which yields $\Gamma_L/\Gamma_U=(1.80\pm0.50)$ [20]. The experimental partial semileptonic widths $\Gamma(D^+\to K^{*0}e^+\nu)=(2.85\pm0.54)\times10^{-14}\,\text{GeV}$ and $\Gamma(D^0\to K^{*-}e^+\nu)=(2.62\pm0.56)\times10^{-14}\,\text{GeV}$ (nonresonant background $(0.32\pm0.25)\times10^{-14}\,\text{GeV}$ and $(0.31\pm0.22)\times10^{-14}\,\text{GeV}$, respectively) [18] agree with our results, since we adjusted $I=0.5$. Depending on the model the nonresonant background is between 6% and 36%. The zero-width model deviates from the full width model by approximately 10% in agreement with earlier findings [7]. This is also true for the asymmetries $(T, I\sin 2\theta^*, P, A\sin 2\theta^*)$ in Table 1. Since the additional $K_0^*(1430)$ resonance makes a contribution only in the amplitude f, the decay rates Γ_U, Γ_T and Γ_P must be equal for the three models with varying s-wave ($\varepsilon=0,\pm1$). All

Table 1. The total decay width $\Gamma_{U+L}(=U+L)$ and the partial decay width Γ_i in units of 10^{-14} GeV, the ratio $\Gamma_L/\Gamma_U(=L/U)$ and the parameter α for various choices of input parameters in the model with $I=0.5$, $R_{12}=0$, $R_V=1.86$

	Pure K^* resonance		Incl. D^* res.	Background, and K_0^* res.		
	Zero width	Full width		$\varepsilon=0$	$\varepsilon=-1$	$\varepsilon=+1$
$U+L$	3.153	2.857	3.173	3.334	3.305	4.098
$(1+\alpha)/2$	1.79	1.78	1.52	1.46	1.19	1.20
L/U	1.79	1.80	1.96	2.00	1.97	2.69
U	1.132	1.020	1.071	1.112	1.112	1.112
L	2.021	1.837	2.102	2.222	2.193	2.986
T	−0.392	−0.355	−0.325	−0.317	−0.317	−0.317
V	0.	0.	−0.079	−0.111	−0.111	−0.111
F	0.	0.	0.076	0.082	0.085	0.080
$F\sin 2\theta^*$	0.	0.	0.054	0.072	0.075	0.070
I	0.	0.009	−0.025	−0.008	−0.023	0.010
$I\sin 2\theta^*$	0.496	0.446	0.439	0.447	0.447	0.446
P	0.778	0.697	0.712	0.671	0.671	0.671
A	0.	0.004	−0.086	−0.122	−0.061	−0.183
$A\sin 2\theta^*$	0.225	0.202	0.187	0.173	0.178	0.169
N	0.	0.	0.137	0.150	0.064	0.235
$N\sin 2\theta^*$	0.	0.	0.015	0.015	0.015	0.014

partial decay rates, where f is present, i.e. $\Gamma_L, \Gamma_F, \Gamma_I, \Gamma_A$ and Γ_N (and their moments with $\sin 2\theta^*$) change when ε is varied. Those angular coefficients which do not vanish for the pure resonance model are not changed appreciably when background terms are added as is seen by comparing the results in the lines for $U, L, T, I\sin 2\theta^*, P$ and $A\sin 2\theta^*$. Most interesting are those angular coefficients which vanish for the pure resonance model, since they involve imaginary parts, i.e. Γ_V, Γ_F and Γ_N, and which, without interference of several $K\pi$ partial waves with different strong interaction phases are signals for CP violation [1]. The larger ones, i.e. Γ_V and Γ_N, are approximately 5% compared to Γ_{U+L}. This means any CP violation in the decay $D \to K^* l\nu$ must be very large if it should be visible in these asymmetry parameters. Since we rather expect that CP violating amplitudes, if they exist at all, are only a very small fraction of the CP conserving contributions, it is hopeless to detect direct CP violation in asymmetries for semileptonic D decays to $K\pi$ final states.

In order to get more information how the various asymmetries depend on input parameters, in particular on the form factors F_2^A and F^V, we made an additional evaluation for the canonical values in (28), i.e. for $R_{12}=R_V=1$. The results are exhibited in Table 2. We kept $I=0.5$, in order to make the comparison of the results in Tables 1 and 2 easier. The major changes occur in the ratio L/U. This is directly connected with the increase of R_{12}. Second P is reduced, which is related to the reduction of R_V. As was mentioned earlier that if the pure resonance model is the correct one, the data of E691 prefer the parameters, which were used in Table 1. For the other more complicated models which include background contributions of various kinds a new fit to the data must be made, since in the analysis of the data only pure resonance contributions were assumed.

Of course we get more information on the difference of our five models by looking at distributions of the $\Gamma_i (i=U, L, T$ etc.) in the remaining variables s_{23}, θ^* and q^2. Since we cannot plot the dependence on all the three variables simultaneously we decided to show only one distribution in s_{23}, namely the one of Γ_{U+L} and various q^2 distributions. To limit the number of figures we have done this only for the models with parameters as in Table 1. The results of the $m_{23}=\sqrt{s_{23}}$ distribution are exhibited in Fig. 2a, b. There we show the invariant mass distribution $d\Gamma_{U+L}/dm_{23}$ for the five models, pure K^*, K^*+D^*, K^*+D^* with $\varepsilon=0, \pm 1$ for comparison in logarithmic and in linear scale. In all models the decay rate away from the K^* peak is almost two orders of magnitude smaller than at the peak and presumably still compatible with the published mass distributions of E691

	Pure K^* resonance		Incl. D^* res.	Background, and K_0^* res.		
	Zero width	Full width		$\varepsilon=0$	$\varepsilon=-1$	$\varepsilon=+1$
$U+L$	2.183	1.975	2.385	2.569	2.505	3.368
$(1+\alpha)/2$	1.16	1.17	0.99	0.94	0.95	0.82
L/U	1.16	1.17	1.48	1.52	1.46	2.30
U	1.009	0.910	0.962	1.019	1.019	1.019
L	1.174	1.065	1.423	1.549	1.485	2.349
T	−0.454	−0.410	−0.379	−0.363	−0.363	−0.363
V	0.	0.	−0.085	−0.121	−0.121	−0.121
F	0.	0.	0.044	0.047	0.071	0.024
$F\sin 2\theta^*$	0.	0.	0.042	0.059	0.061	0.057
I	0.	0.007	−0.028	−0.008	−0.024	0.009
$I\sin 2\theta^*$	0.397	0.358	0.350	0.358	0.358	0.357
P	0.418	0.375	0.389	0.344	0.344	0.344
A	0.	0.001	−0.094	−0.141	−0.073	−0.210
$A\sin 2\theta^*$	0.094	0.084	0.070	0.054	0.058	0.049
N	0.	0.	0.136	0.149	0.063	0.234
$N\sin 2\theta^*$	0.	0.	0.012	0.014	0.015	0.013

Table 2. The total decay width $\Gamma_{U+L}(=U+L)$ and the partial decay width Γ_i in units of 10^{-14} GeV, the ratio $\Gamma_L/\Gamma_U(=L/U)$ and the parameter α for various choices of input parameters in the model with $I=0.5$, $R_{12}=1$, $R_V=1$

[10]. Further checks would require the application of cuts and other corrections to our model decay rates which is beyond the purpose of this paper.

Next we have calculated the q^2 dependence of the angular coefficients. We have integrated over s_{23} and θ^* and have calculated $d\Gamma_i/dq^2$ for all $i=U, L, T$ etc. and for five models. The results are shown in Fig. 3–15. For the pure resonance model we also show the curves in zero-width approximation. Thus there are maximally six curves in every figure. In some of the plots the pure resonance model give vanishing assymmetries. In others the curves for $\varepsilon=0, \pm 1$ coincide. All $d\Gamma_i/dq^2$ are plotted in units of $10^{-14}\,\mathrm{GeV}^{-1}$. The integrals under the curves are equal to the numbers in Table 1. For U, T and V the curves for $\varepsilon=0, \pm 1$ coincide since the K_0^* term influences only the amplitude f as we explained already above. Those decay distributions which are not zero for the pure K^* resonance model, namely $U, L, T, I\sin 2\theta^*, P, A\sin 2\theta^*$ do not differ qualitatively very much if we compare all five models. The only exception is $d\Gamma_L/dq^2$ which shows strong changes in the behaviour for small q^2 if a K_0^* term with $\varepsilon=1$ is considered. Thus $d\Gamma_L/dq^2$ can be considered as good indicator for additional K_0^* contributions which might not be visible strongly enough in the invariant mass distribution.

At this point we must emphasize that the partial decay distributions $d\Gamma_i$ are defined as in (15) on the basis of the factorization of the θ and χ dependence in terms of the factors l_i defined in (12). This differs from other definitions [12–14], where also the dependence on the meson decay angle is factored out. However, the θ^* dependence is simple and explicit and factorizable only for the pure K^* resonance model (with no off-mass-shell terms). The models with background ($\varepsilon=0, \pm 1$) on the other hand have a different $\cos\theta^*$ dependence than the pure resonance model, in particular $d\Gamma_L$ has not the characteristic factor $\cos^2\theta^*$ as the pure K^* resonance model has but has the more complicated $\cos\theta^*$ dependence of the form $|a+b\cos\theta^*|^2$. The constant term $|a|^2$ contributes with a larger term when we integrate over $\cos\theta^*$ compared to a term that has the additional $\cos^2\theta^*$ factor. Therefore the K_0^* resonance terms which mostly contribute to a have a particularly large effect in $d\Gamma_L/dq^2$ (see Fig. 3). The effect of the θ^* independent term a is also seen quite clearly in Fig. 9 ($d\Gamma_I/dq^2$) and in Fig. 12 ($d\Gamma_A/dq^2$) whereas in Figs. 10 and 13 ($I\sin 2\theta^*$ and $A\sin 2\theta^*$) we see the change of the background models ($\varepsilon=0, \pm 1$) compared to the pure resonance model which has the characteristic factor $\sin 2\theta^*$ in $d^3\Gamma_I$ and $d^3\Gamma_A$. The decay rates which are proportional to imaginary parts are exhibited in Figs. 6, 7, 8, 14 and 15. They are definitely nonnegligible. In order to determine the various coefficients $d^3\Gamma_i(i=U, L, T$ etc.) in the charged lepton angular distribution from experiment a

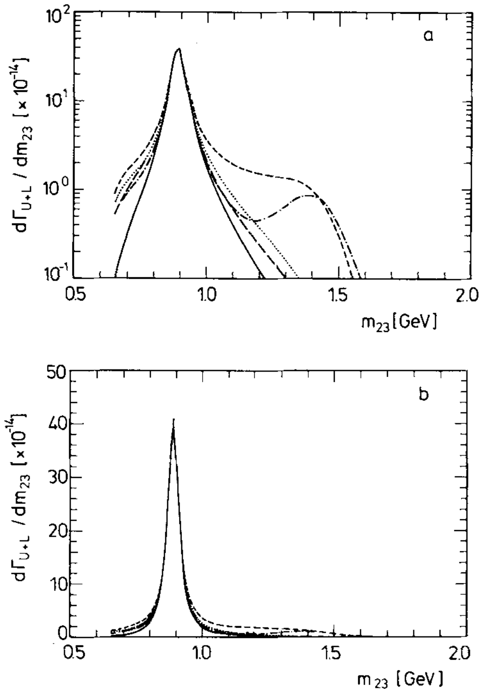

Fig. 2 a, b. $K\pi$ invariant mass distribution $d\Gamma_{U+L}/dm_{23}$ as a function of m_{23} for five models: pure K^* resonance with finite width (full line), K^* and D^* resonance (long dashed), K^*, D^* and background, $\varepsilon = 0$ (dotted), K^*, D^*, K_0^* and background for $\varepsilon = -1$ (dashed-dotted) and for $\varepsilon = 1$ (short dashed). **a** logarithmic plot, **b** linear plot

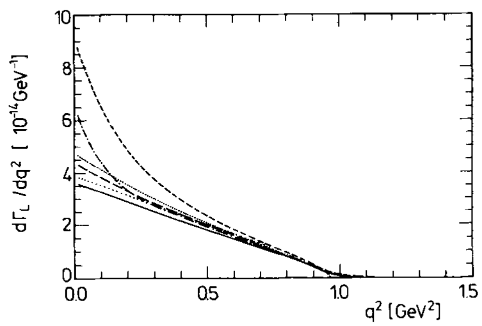

Fig. 3. $d\Gamma_L/dq^2$ as a function of q^2 for six models: pure K^* resonance in zero-width approximation (very short dashed), all other curves labelled as in Fig. 2

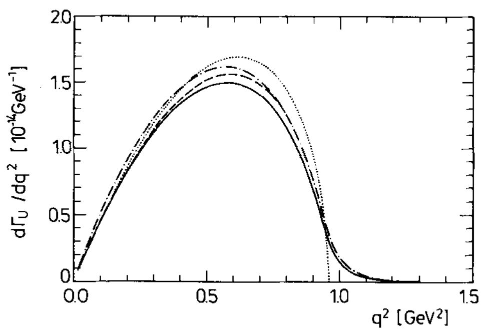

Fig. 4. $d\Gamma_U/dq^2$ as a function of q^2 for six models labelled as in Fig. 3. The curves for $\varepsilon = 0, \pm 1$ coincide

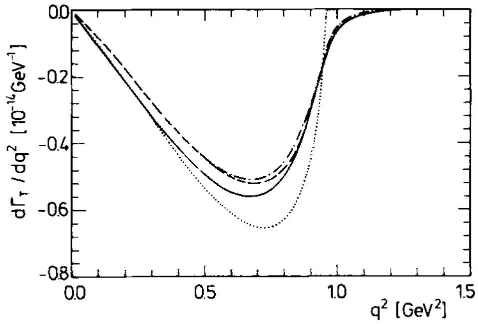

Fig. 5. $d\Gamma_T/dq^2$ as a function of q^2 for six models labelled as in Fig. 3. The curves for $\varepsilon = 0, \pm 1$ coincide

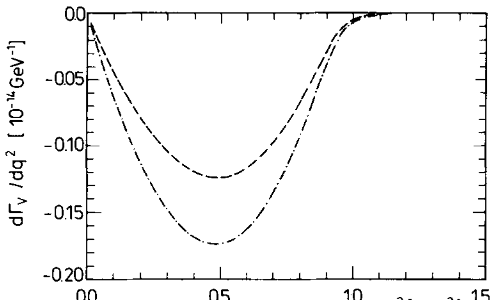

Fig. 6. $d\Gamma_V/dq^2$ as a function of q^2 for six models labelled as in Fig. 3. The curves for $\varepsilon = 0, \pm 1$ coincide. Pure K^* resonance models give $d\Gamma_V = 0$

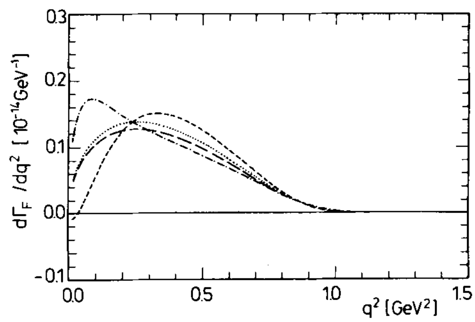

Fig. 7. $d\Gamma_F/dq^2$ as a function of q^2 for six models labelled as in Fig. 3. Pure K^* resonance models give $d\Gamma_F = 0$

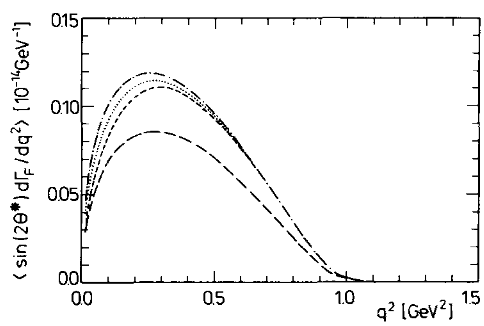

Fig. 8. Same as Fig. 7 with extra factor $\sin 2\theta^*$ in the θ^* integrand

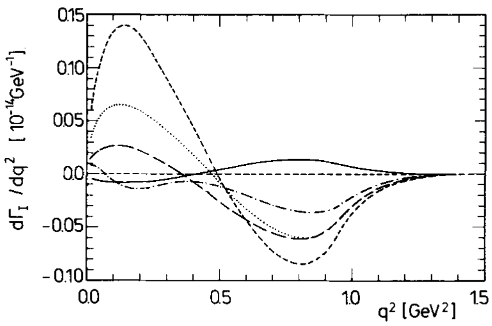

Fig. 9. $d\Gamma_I/dq^2$ as a function of q^2 for six models labelled as in Fig. 3

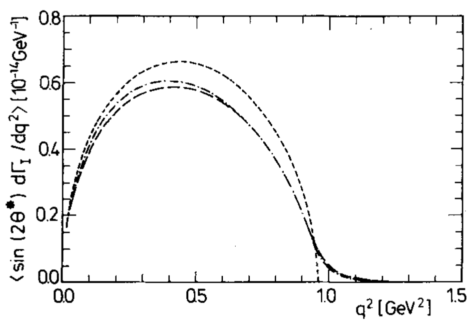

Fig. 10. Same as Fig. 9 with extra factor $\sin 2\theta^*$ in the θ^* integrand

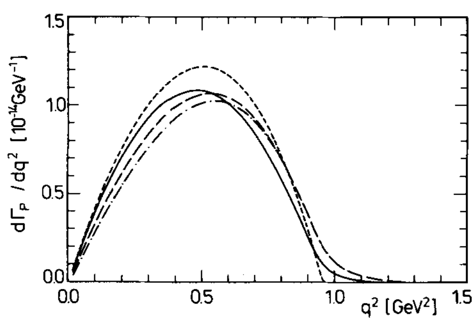

Fig. 11. $d\Gamma_P/dq^2$ as a function of q^2 for six models labelled as in Fig. 3. The curves for $\varepsilon = 0, \pm 1$ coincide

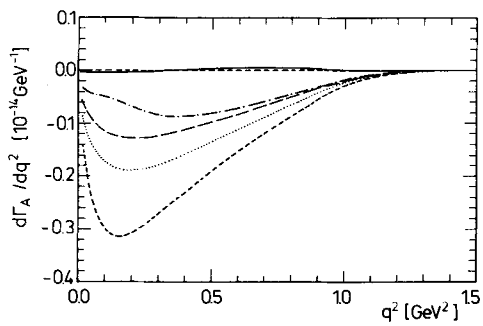

Fig. 12. $d\Gamma_A/dq^2$ as a function of q^2 for six models labelled as in Fig. 3

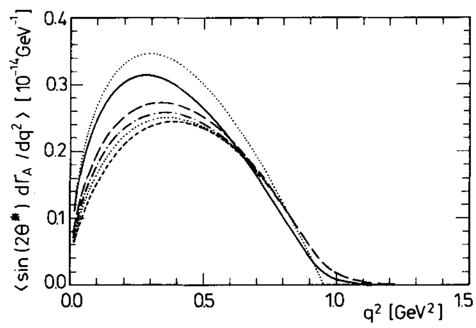

Fig. 13. Same as Fig. 12 with extra factor $\sin 2\theta^*$ in the θ^* integrand

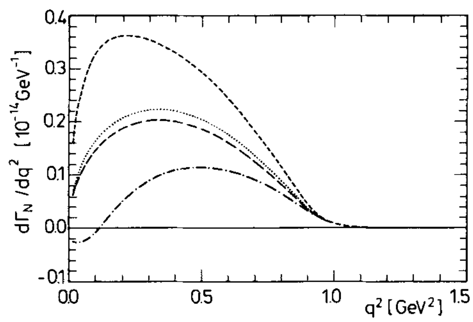

Fig. 14. $d\Gamma_N/dq^2$ as a function of q^2 for six models labelled as in Fig. 3

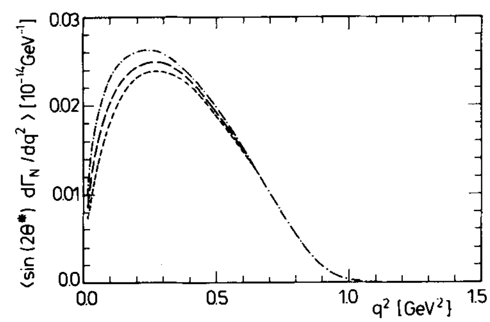

Fig. 15. Same as Fig. 14 with extra factor $\sin 2\theta^*$ in the θ^* integrand

combined fit of the $\theta, \chi, \theta^*, s_{23}$ and q^2 dependence must be performed by which, with sufficient data, all nine coefficient functions $d^3\Gamma_i$ in the combined angular correlation (15) will be obtained.

5 Summary and conclusions

We have constructed a complete formalism for analysing the semileptonic decay of a pseudoscalar meson into two pseudoscalar mesons, general enough to accommodate various partial waves in the final hadron channel, as well as cross channel poles and backgrounds. We also show how to extend the formalism to the case when lepton masses can not be neglected.

We have presented numerical results for two models in the form of the various invariant decay functions, integrated over q^2 and the final state hadron mass distribution. From these all angular correlations can be constructed. We have also illustrated the q^2 dependence and the hadron mass distribution for selected decay functions and moments.

Current data from Fermilab Experiment E691 are too crude definitively to distinguish between the two models. The superior fit of our Table 1 compared to Table 2 does however suggest that the canonical quark model may have difficulty in describing $D \to K^* e\nu$ angular correlations.

Appendix A: basis tensors

In this appendix we write down the nine basis tensors $L_{\mu\nu}^{(i)}(i = U, L, T, V, F, I, P, A, N)$, which are defined in (7). Their space components ($\mu, \nu = 1, 2, 3$) are:

$$L^{(U)} = \begin{pmatrix} 1 & 0 & 0 \\ 0 & 1 & 0 \\ 0 & 0 & 0 \end{pmatrix} \qquad L^{(F)} = \frac{1}{2\sqrt{2}} \begin{pmatrix} 0 & 0 & 0 \\ 0 & 0 & -1 \\ 0 & -1 & 0 \end{pmatrix}$$

$$L^{(L)} = \begin{pmatrix} 0 & 0 & 0 \\ 0 & 0 & 0 \\ 0 & 0 & 1 \end{pmatrix} \qquad L^{(I)} = \frac{1}{2\sqrt{2}} \begin{pmatrix} 0 & 0 & 1 \\ 0 & 0 & 0 \\ 1 & 0 & 0 \end{pmatrix}$$

$$L^{(T)} = \frac{1}{2} \begin{pmatrix} -1 & 0 & 0 \\ 0 & 1 & 0 \\ 0 & 0 & 0 \end{pmatrix} \qquad L^{(P)} = \begin{pmatrix} 0 & i & 0 \\ -i & 0 & 0 \\ 0 & 0 & 0 \end{pmatrix}$$

$$L^{(V)} = \frac{1}{2} \begin{pmatrix} 0 & 1 & 0 \\ 1 & 0 & 0 \\ 0 & 0 & 0 \end{pmatrix} \qquad L^{(A)} = \frac{1}{2\sqrt{2}} \begin{pmatrix} 0 & 0 & 0 \\ 0 & 0 & -i \\ 0 & i & 0 \end{pmatrix}.$$

$$L^{(N)} = \frac{1}{2\sqrt{2}} \begin{pmatrix} 0 & 0 & -i \\ 0 & 0 & 0 \\ i & 0 & 0 \end{pmatrix} \tag{40}$$

The four-momenta k and k' are given in (8) in terms of the angles θ and χ. With these we write the lepton tensor in terms of q^2 and these angles. With the help of the explicit form of the basis tensors given above it is a simple exercise to calculate the coefficient functions l_U, l_L, l_T etc. as defined in (6). The result is written in (12).

Appendix B: non-zero charged lepton mass

In this appendix we present the changes that occur when the mass of the charged lepton is unequal zero. This will be relevant when the accuracy of the experimental data improves so that differences between D decays into electrons and muons become visible.

For $m_l \neq 0$ the lepton tensor in (6) will depend on the charged lepton mass. Furthermore we have an additional polarization vector $\varepsilon^\mu(q, s) = q^\mu/\sqrt{q^2}$ so that the tensors $L_{\mu\nu}^{\rho\sigma}$ defined in (5) have also time components. Also the lepton tensor $l_{\mu\nu}$ has time components now. The space components ($\mu, \nu = 1, 2, 3$) can still be decomposed as in (6) and the matrices $L^{(i)}(i = U, L, T,$ etc.) are still in the form as given in Appendix A. The coefficients $l_U, l_L, l_T, l_V,$ etc. change and are now:

$$l_U = \tfrac{3}{8}(1 - \Delta_l)(1 + \cos^2\theta + \Delta_l \sin^2\theta)$$

$$l_F = \frac{3}{2\sqrt{2}}(1 - \Delta_l)^2 \sin 2\theta \sin\chi$$

$$l_L = \tfrac{3}{4}(1 - \Delta_l)(\sin^2\theta + \Delta_l \cos^2\theta)$$

$$l_I = -\frac{3}{2\sqrt{2}}(1 - \Delta_l)^2 \sin 2\theta \cos\chi$$

$$l_T = \tfrac{3}{4}(1 - \Delta_l)^2 \sin^2\theta \cos 2\chi$$

$$l_N = \frac{3}{\sqrt{2}}(1 - \Delta_l) \sin\theta \sin\chi$$

$$l_V = -\tfrac{3}{4}(1 - \Delta_l)^2 \sin^2\theta \sin 2\chi$$

$$l_A = -\frac{3}{\sqrt{2}}(1 - \Delta_l) \sin\theta \cos\chi$$

$$l_P = \tfrac{3}{4}(1 - \Delta_l)\cos\theta \tag{41}$$

where $\Delta_l = m_l^2/q^2$. In addition to the tensors (7) we have now the tensors involving the polarization vector $\varepsilon(q, s)$. They are:

$$\begin{aligned} &L^{(ss)} = L^{ss} \\ &L^{(01)} = L^{s+} - L^{s-} \qquad L^{(10)} = L^{+s} - L^{-s} \\ &L^{(02)} = L^{s+} + L^{s-} \qquad L^{(20)} = L^{+s} + L^{s-} \\ &L^{(s0)} = L^{s0} \qquad\qquad L^{(0s)} = L^{0s}. \end{aligned} \tag{42}$$

The corresponding matrices are:

$$L^{(ss)} = \begin{pmatrix} 1 & 0 & 0 & 0 \\ 0 & 0 & 0 & 0 \\ 0 & 0 & 0 & 0 \\ 0 & 0 & 0 & 0 \end{pmatrix}$$

$$L^{(s0)} = \begin{pmatrix} 0 & 0 & 0 & 1 \\ 0 & 0 & 0 & 0 \\ 0 & 0 & 0 & 0 \\ 0 & 0 & 0 & 0 \end{pmatrix} \qquad L^{(0s)} = \begin{pmatrix} 0 & 0 & 0 & 0 \\ 0 & 0 & 0 & 0 \\ 0 & 0 & 0 & 0 \\ 1 & 0 & 0 & 0 \end{pmatrix}$$

$$L^{(01)} = \sqrt{2} \begin{pmatrix} 0 & 1 & 0 & 0 \\ 0 & 0 & 0 & 0 \\ 0 & 0 & 0 & 0 \\ 0 & 0 & 0 & 0 \end{pmatrix} \qquad L^{(10)} = \sqrt{2} \begin{pmatrix} 0 & 0 & 0 & 0 \\ 1 & 0 & 0 & 0 \\ 0 & 0 & 0 & 0 \\ 0 & 0 & 0 & 0 \end{pmatrix}$$

$$L^{(02)} = \sqrt{2} \begin{pmatrix} 0 & 0 & 1 & 0 \\ 0 & 0 & 0 & 0 \\ 0 & 0 & 0 & 0 \\ 0 & 0 & 0 & 0 \end{pmatrix} \qquad L^{(20)} = \sqrt{2} \begin{pmatrix} 0 & 0 & 0 & 0 \\ 0 & 0 & 0 & 0 \\ -1 & 0 & 0 & 0 \\ 0 & 0 & 0 & 0 \end{pmatrix}. \tag{43}$$

With the help of these tensors we decompose the lepton tensor restricted to time components (μ and/or $\nu = 0$) as follows:

$$\begin{aligned} l_{\mu\nu} = \frac{2q^2}{3}\{&K_{00} L_{\mu\nu}^{(ss)} + K_{01}(L_{\mu\nu}^{(01)} + L_{\mu\nu}^{(10)}) \\ &+ K_{02}(L_{\mu\nu}^{(02)} - L_{\mu\nu}^{(20)}) + K_{s0}(L_{\mu\nu}^{(0s)} + L_{\mu\nu}^{(s0)})\}. \end{aligned} \tag{44}$$

The coefficients $K_{\rho\sigma}$ are expressed by the angles θ and χ and by Δ_l:

$$
\begin{aligned}
&K_{00} = \tfrac{3}{4}\Delta_l(1-\Delta_l)\\
&K_{01} = K_{10} = -\tfrac{1}{4}\Delta_l(1-\Delta_l)l_A\\
&K_{02} = -K_{20} = \tfrac{1}{4}\Delta_l(1-\Delta_l)l_N\\
&K_{0s} = K_{s0} = \Delta_l(1-\Delta_l)l_P
\end{aligned} \tag{45}
$$

where l_A, l_N, l_P are defined in (11), which are the angular factors for the case $m_l=0$. In addition to H_i with $i=U,L,T,V,F,I,P,A,N$ we have now also H_i with $i=(ss),(01),(10),(02),(20),(s0),(0s)$ which are obtained from (9) by multiplying $H_{\mu\nu}$ with the appropriate polarization tensors, i.e.

$$
\begin{aligned}
&H_{(ss)} = H^{ss}\\
&H_{(01)} = -\tfrac{1}{4}(H^{s+}-H^{s-}) \quad H_{(10)} = -\tfrac{1}{4}(H^{+s}-H^{-s})\\
&H_{(02)} = -\tfrac{1}{4}(H^{s+}+H^{s-}) \quad H_{(20)} = \tfrac{1}{4}(H^{+s}+H^{s-})\\
&H_{(s0)} = H^{s0} \qquad\qquad\qquad H_{(0s)} = H^{0s}.
\end{aligned} \tag{46}
$$

The tensor product $l^{\mu\nu}H_{\mu\nu}$ in (10) gets also additional terms. They are all proportional to $\Delta_l(1-\Delta_l)$:

$$
\begin{aligned}
&(l^{\mu\nu}H_{\mu\nu})_{\text{add. terms}}\\
&\quad = \Delta_l(1-\Delta_l)[H_{(ss)}(l_U+\tfrac{1}{2}l_L)+l_A(H_{(01)}+H_{(10)})\\
&\qquad + l_N(H_{(02)}+H_{(20)})+l_P(H_{(s0)}+H_{(0s)})]
\end{aligned} \tag{47}
$$

where l_U, l_L, l_A, l_N, l_P are again the angular factors defined in (11) for $m_l=0$, so that in (47) the same angular factors appear as in (11). The matrix elements, of course, are different. This means that with $\Delta_l \neq 0$ one has the same decomposition into angular factors as for $\Delta_l=0$. The only difference is that Δ_l dependent terms and additional structure functions like $H_{(01)}$ etc. appear.

For calculating these new structure functions we need the projection of the current matrix element (16) on the polarization vector $\varepsilon(q,s)$. This is

$$
\begin{aligned}
F_s &= \varepsilon^*(q,s)_\mu J^\mu\\
&= \frac{1}{m_1\sqrt{q^2}}(Pqf+[\kappa Pq+\sqrt{a_2}X\cos\theta^*]g+rq^2).
\end{aligned} \tag{48}
$$

Together with (18) it is easy to write down the new structure functions $H_{(01)}$ etc. Since we have not used them for getting the results of this paper we shall refrain from giving their explicit expressions. In order to evaluate them for the model defined in Sect. 3 we need also the function r in this model. This is:

$$
r = f - \frac{i\sqrt{2}m_1}{3F_\pi}G_A\,\mathrm{Res}(D^*). \tag{49}
$$

References

1. A. Pais, S.B. Treiman: Phys. Rev. 168 (1968) 1858 and the earlier literature cited in this reference
2. G. Altarelli et al.: Nucl. Phys. B208 (1982) 365
3. B. Grinstein, A. Isgur, M.B. Wise: Phys. Rev. Lett. 56 (1986) 298; B. Grinstein, N. Isgur, D. Scora, M.B. Wise: Phys. Rev. D39 (1989) 799
4. M. Bauer, B. Stech, M. Wirbel: Z. Phys. C – Particles and Fields 29 (1985) 637
5. T. Altomari, L. Wolfenstein: Phys. Rev. Lett. 58 (1987) 1583; Phys. Rev. D37 (1988) 681
6. J.G. Körner, G.A. Schuler: Z. Phys. C – Particles and Fields 38 (1988) 511
7. J.M. Cline, W.F. Palmer, G. Kramer: Phys. Rev. D40 (1989) 793
8. M. Bauer, M. Wirbel: Z. Phys. C – Particles and Fields 42 (1989) 671; M. Wirbel: Progr. Part. Nucl. Phys. 21 (1988) 33
9. D. Scora, N. Isgur: Phys. Rev. D40 (1989) 1491
10. J.C. Anjos et al.: Phys. Rev. Lett. 62 (1989) 125; 62 (1989) 722; 62 (1989) 1587
11. J.M. Izen: SLAC preprint SLAC-PUB-4753 (1988) unpublished; J. Adler et al.: Phys. Rev. Lett. 62 (1989) 1821
12. F.J. Gilman, R.L. Singleton: SLAC preprint SLAC-PUB-5065 (1989) unpublished
13. J.G. Körner, G.A. Schuler: Z. Phys. C – Particles and Fields 46 (1990) 93
14. K. Hagiwara, A.D. Martin, M.F. Wada: Phys. Lett. B228 (1989) 144; Nucl. Phys. B327 (1989) 569
15. S.-C. Chao, G. Kramer, W.F. Palmer, S. Pinsky: Phys. Rev. D30 (1984) 1916
16. Particle Data Group: Phys. Lett. B204 (1988) 107
17. D. Aston et al.: Nucl. Phys. B296 (1988) 493
18. R. Morrison: DESY Report No T-88-01 (1988) (unpublished)
19. G. Kramer, W.F. Palmer: Phys. Rev. D36 (1987) 154
20. Talk presented by J. Dubosq at the Division of Particles and Fields Meeting of the American Physical Society, Houston, Texas, January 1990
21. P. Avery et al.: Cornell preprint CLNS 89/939, CLEO 89-11 (unpublished)